

# Production and Release of Molecular Bromine and Chlorine from the Arctic Coastal Snowpack

K. D. Custard,<sup>†</sup> A. R. W. Raso,<sup>†</sup> P. B. Shepson,<sup>†,‡</sup> R. M. Staebler,<sup>§</sup> and K. A. Pratt\*,<sup>¶,||</sup> 

<sup>†</sup>Department of Chemistry and <sup>‡</sup>Department of Earth, Atmospheric, and Planetary Sciences and Purdue Climate Change Research Center, Purdue University, West Lafayette, Indiana 47907, United States

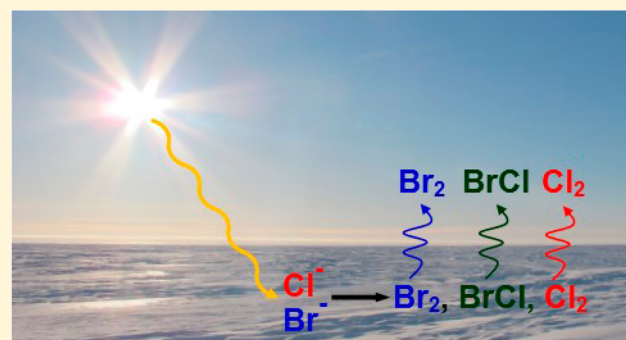
<sup>§</sup>Air Quality Processes Section, Environment and Climate Change Canada, Toronto, Ontario M3H 5T4, Canada

<sup>¶</sup>Department of Chemistry and Department of Earth and Environmental Sciences, University of Michigan, Ann Arbor, Michigan 48109, United States

## Supporting Information

**ABSTRACT:** Atmospheric bromine and chlorine atoms have a significant influence on the pathways of atmospheric chemical species processing. The photolysis of molecular halogens and subsequent reactions with ozone, mercury, and hydrocarbons are common occurrences in the Arctic boundary layer during spring, following polar sunrise. While it was recently determined that  $\text{Br}_2$  is released from the sunlit surface snowpack, the source(s) and mechanisms of  $\text{Cl}_2$  and  $\text{BrCl}$  production have remained unknown. Current efforts to model Arctic atmospheric composition are limited by the lack of knowledge of the sources and emission rates of these species. Here, we present the first simultaneous direct measurements of  $\text{Br}_2$ ,  $\text{Cl}_2$ , and  $\text{BrCl}$  in snowpack interstitial air, as well as the first measured emission rates of  $\text{Br}_2$  and  $\text{Cl}_2$  out of the snowpack into the atmosphere. Using chemical ionization mass spectrometry,  $\text{Br}_2$ ,  $\text{Cl}_2$ , and  $\text{BrCl}$  were observed to be produced within the tundra surface snowpack near Utqiagvik, AK, during Feb 2014, following both artificial and natural irradiation, consistent with a photolytic production mechanism. Maximum  $\text{Cl}_2$  and  $\text{Br}_2$  fluxes from the snowpack to the overlying atmosphere were quantified and reached maxima at mid-day during peak radiation. In-snowpack  $\text{Br}_2$  and  $\text{BrCl}$  production was enhanced, with  $\text{Cl}_2$  production reduced, at air temperatures below the eutectic point for the formation of  $\text{NaCl} \cdot 2\text{H}_2\text{O}$ , suggesting limited chloride availability, as compared to production at air temperatures above this eutectic point. These new observations improves the ability of the community to simulate Arctic boundary layer composition and pollutant fate.

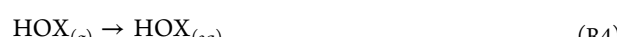
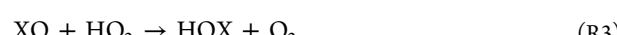
**KEYWORDS:** snowpack, atmosphere, flux, photochemistry, ozone, mass spectrometry, Utqiagvik, Alaska



## 1. INTRODUCTION

Halogen chemistry has been widely studied throughout the Arctic over the past several decades.<sup>1,2</sup> Bromine, in particular, has been linked with ozone depletion events (ODEs), when ozone drops from background levels of 40 ppb (nmol/mol) to below 5 ppb.<sup>3,4</sup> This has been shown to occur sporadically during the Arctic springtime.<sup>5</sup> Because most of these measurements took place at coastal locations, sea salt was proposed as one of the important sources of atmospheric molecular halogens.<sup>6</sup> It was hypothesized that acidic aerosols provided the initial release and a surface for heterogeneous recycling of atmospheric  $\text{Br}_2$  to occur during ODEs.<sup>6,7</sup> However, modeling studies have shown that heterogeneous recycling of bromine species on the surface snowpack results in simulated  $\text{O}_3$  depletion rates that match observations.<sup>8–10</sup> The snowpack surface is open to deposition of sea salt aerosol, acids, and reactive bromine species (e.g.,  $\text{HOBr}$  and  $\text{BrONO}_2$ ), which can lead to the production of molecular halogens.<sup>11</sup>

Pratt et al.<sup>12</sup> showed that the Arctic surface snowpack (near Utqiagvik, AK) can produce molecular bromine ( $\text{Br}_2$ ) in the presence of solar radiation, and this production is enhanced by an increase in the  $\text{O}_3$  concentration as a result of heterogeneous chemistry, as shown in the general reactions R1–R8.<sup>1</sup>



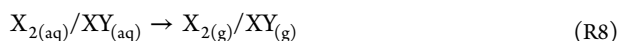
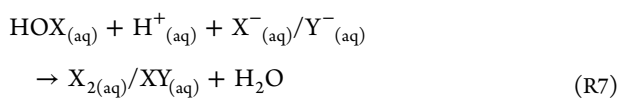
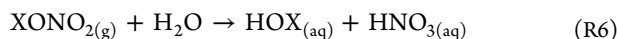
Received: February 17, 2017

Revised: April 10, 2017

Accepted: April 12, 2017

Published: April 12, 2017





The observed  $\text{Br}_2$  surface snowpack production is consistent with elevated  $\text{Br}_2$  observed in the surface snowpack interstitial air in early March at Alert, Nunavut, Canada.<sup>13</sup> Lower tropospheric  $\text{Br}_2$  has been observed at up to 27 ppt from February to early March at Alert<sup>13,14</sup> and up to 46 ppt in March–April near Utqiagvik, AK.<sup>15</sup> While  $\text{BrCl}$  and  $\text{Cl}_2$  were not observed in the snow chamber experiments by Pratt et al.,<sup>12</sup>  $\text{BrCl}$  has been observed at up to 35 ppt at Alert<sup>13,14</sup> and up to 14 ppt near Utqiagvik,<sup>16</sup> and  $\text{Cl}_2$  has been observed at up to 400 ppt near Utqiagvik.<sup>16,17</sup> Current models are limited by the lack of understanding of the sources and emission rates of molecular halogens, especially for  $\text{BrCl}$  and  $\text{Cl}_2$ , which impact the fate of volatile organic compounds through faster oxidation by Cl atoms than by the hydroxyl radical.<sup>18</sup> This information is crucial to properly simulate future Arctic atmospheric composition,<sup>19</sup> especially given rapid sea ice surface change.<sup>20</sup>

To further investigate the tundra snowpack as a source of  $\text{Cl}_2$  and  $\text{BrCl}$ , we deployed chemical ionization mass spectrometry (CIMS) near Utqiagvik, AK during Feb 2014 to perform real-time measurements of gas-phase inorganic halogens within the interstitial snowpack air. Sunlit and artificial light experiments were conducted to investigate the impact of photochemical reactions on snowpack halogen chemistry, including production of  $\text{Br}_2$ ,  $\text{Cl}_2$ , and  $\text{BrCl}$ . Vertical profile experiments were conducted above the surface snowpack to determine the fluxes of  $\text{Br}_2$  and  $\text{Cl}_2$  from the snowpack.

## 2. EXPERIMENTAL SECTION

**2.1. Measurements.** In-snowpack and vertical profile measurements of  $\text{Br}_2$ ,  $\text{Cl}_2$ , and  $\text{BrCl}$  were conducted using CIMS during Feb 2014 near Utqiagvik, AK ( $71^\circ 16.500\text{ N}$ ,  $156^\circ 38.426\text{ W}$ ). Simultaneous  $\text{O}_3$  concentration measurements were performed using a 2B Technologies model 205 dual-beam  $\text{O}_3$  monitor. Meteorological variables were measured at sites located 5 km upwind of the CIMS field site, with only flat tundra present between the sites. Wind direction, wind speed, and temperature data at 10 m were obtained from the National Oceanic and Atmospheric Administration (NOAA) Barrow Observatory (<http://www.esrl.noaa.gov/gmd/obop/brw/>), and down-welling radiation data were obtained from the Atmospheric Radiation Measurement Climate Research Facility (<https://www.arm.gov/capabilities/observatories/nsa>). Melted surface snow pH and inorganic ion concentrations were measured for snow collected on Feb 5, 23, and 28, 2014, as detailed in the *Supporting Information* and shown in **Table S1** of the *Supporting Information*.

CIMS with  $\text{I}(\text{H}_2\text{O})_n^-$  reagent ions monitored  $\text{Br}_2$  as  $\text{I}^{79}\text{Br}^{79}\text{Br}^-$  (285 amu),  $\text{I}^{79}\text{Br}^{81}\text{Br}^-$  (287 amu), and  $\text{I}^{81}\text{Br}^{81}\text{Br}^-$  (289 amu).<sup>15</sup>  $\text{Cl}_2$  was monitored as  $\text{I}^{35}\text{Cl}^{35}\text{Cl}^-$  (197 amu) and  $\text{I}^{37}\text{Cl}^{35}\text{Cl}^-$  (199 amu), and  $\text{BrCl}$  was monitored as  $\text{I}^{79}\text{Br}^{35}\text{Cl}^-$  (241 amu) and  $\text{I}^{79}\text{Br}^{37}\text{Cl}^-/\text{I}^{81}\text{Br}^{35}\text{Cl}^-$  (243 amu). Each mass was monitored for 500 ms with 6% duty cycles. CIMS has been described previously by Liao et al.<sup>15</sup> and Peterson et al.;<sup>21</sup> therefore, only a brief description will be given here. The CIMS sampled by continuously pulling 8.2 standard liters per minute

(slpm) of ambient air through a custom three-way inlet valve.<sup>22</sup> After the sampled ambient air passes through the inlet valve, 2 slpm of the flow entered the CIMS, 1.3 slpm was directed to the  $\text{O}_3$  monitor for simultaneous measurements, and the remaining flow was removed as exhaust. Hydrated  $\text{I}^-$  clusters,  $(\text{H}_2\text{O})_n\text{I}^-$ , were produced inside the CIMS flow reactor using a 2.0 slpm flow of  $\text{CH}_3\text{I}$  (5 ppm) in  $\text{N}_2$  passed through a  $^{210}\text{Po}$  ionizing source and mixed with a flow of humidified  $\text{N}_2$  inside the flow reactor. Humidified  $\text{N}_2$  was made by flowing  $\text{N}_2$  through room-temperature ( $\sim 26^\circ\text{C}$ ) deionized water housed in a glass bubbler. The water addition ensured that the atmospheric water vapor did not affect the CIMS sensitivity.

Background measurements were performed every 20 min by passing the ambient air through a glass wool scrubber. Previous lab and field studies have shown that glass wool can remove inorganic halogens with high efficiency (>95%).<sup>23</sup> The removal was verified during the field study by adding large concentrations of both  $\text{Cl}_2$  (2500 ppt) and  $\text{Br}_2$  (1500 ppt) into the ambient air sample and passing it through the glass wool scrubber. Both  $\text{Cl}_2$  and  $\text{Br}_2$  were generated from permeation tubes (KIN-TEK), which were also used as calibration standards.

Calibration of  $\text{Br}_2$  and  $\text{Cl}_2$  was performed periodically (typically every 0.5 h) by individually adding a known concentration of either  $\text{Br}_2$  (1500 pptv) or  $\text{Cl}_2$  (2500 pptv) to the ambient air being sampled. The typical  $\text{Br}_2$  (285 amu) and  $\text{Cl}_2$  (197 amu) sensitivities during the in-snowpack experiments (Feb 8–9, 2014) were  $13.6 \pm 0.9$  and  $16.6 \pm 0.9 \text{ Hz ppt}^{-1}$ , respectively, and  $13.5 \pm 0.3$  and  $19.6 \pm 0.9 \text{ Hz ppt}^{-1}$ , respectively, during the vertical profile experiments (Feb 16, 2014), described below. A sensitivity midway between those of  $\text{Br}_2$  and  $\text{Cl}_2$  (20.4 Hz/ppt) was assumed for  $\text{BrCl}$  (243 amu) for the in-snowpack experiments. To account for any minor changes in  $\text{H}_2\text{O}$  addition and detector sensitivity during the study, CIMS signals were normalized by mass 147 [ $\text{I}(\text{H}_2^{18}\text{O})^-$ ]. During the in-snowpack experiments on Feb 8–9, 2014,  $\text{Br}_2$  (285 amu),  $\text{Cl}_2$  (197 amu), and  $\text{BrCl}$  (243 amu)  $3\sigma$  1 min averaged limits of detection (LODs) were 3.6, 1.0, and 2.2 ppt, respectively. Average in-snowpack experiment uncertainties for  $\text{Br}_2$  and  $\text{Cl}_2$  were estimated to be  $\pm 18$  and  $\pm 21\%$ , respectively. During the flux experiments,  $\text{Br}_2$  (285 amu) and  $\text{Cl}_2$  (197 amu)  $3\sigma$  1 min averaged LODs were 1.0 and 0.7 ppt; given a measurement period of 15 min, we estimate the average LODs to be 0.3 and 0.2 ppt, respectively. The typical uncertainties for  $\text{Br}_2$  and  $\text{Cl}_2$  during the flux experiments were estimated to be  $\pm 21$  and  $\pm 30\%$ , respectively.

To confirm the identity of the detected masses, the two isotopes of the same species (i.e., isotopic masses for  $\text{Br}_2$ ,  $\text{Cl}_2$ , and  $\text{BrCl}$ ) were plotted versus one another to enable comparison of the linear regression to their known isotopic ratio. Confirmation of the presence of a specific molecular halogen was achieved when the best fit line had a slope within  $\pm 10\%$  of the isotopic ratio for that specific molecular halogen. For example, for snowpack interstitial air sampling on Feb 11, 2014, the plot of mass  $\text{I}^{81}\text{Br}^{81}\text{Br}^-$  (289 amu) versus mass  $\text{I}^{79}\text{Br}^{79}\text{Br}^-$  (285 amu) shows a best fit line ( $R^2 = 0.997$ ) with a slope of  $0.929 \pm 0.002$  (**Figure S1** of the *Supporting Information*), confirming the presence of two bromine atoms (isotopic ratio of 0.97). Mass  $\text{I}^{37}\text{Cl}^{35}\text{Cl}^-$  (199 amu) versus mass  $\text{I}^{35}\text{Cl}^{35}\text{Cl}^-$  (197 amu) shows a slope of  $0.627 \pm 0.004$  ( $R^2 = 0.935$ ), confirming the presence of two chlorine atoms (**Figure S2** of the *Supporting Information*, with an isotopic ratio of 0.65). Mass  $\text{I}^{79}\text{Br}^{37}\text{Cl}^-$  (243 amu) versus mass  $\text{I}^{79}\text{Br}^{35}\text{Cl}^-$  (241

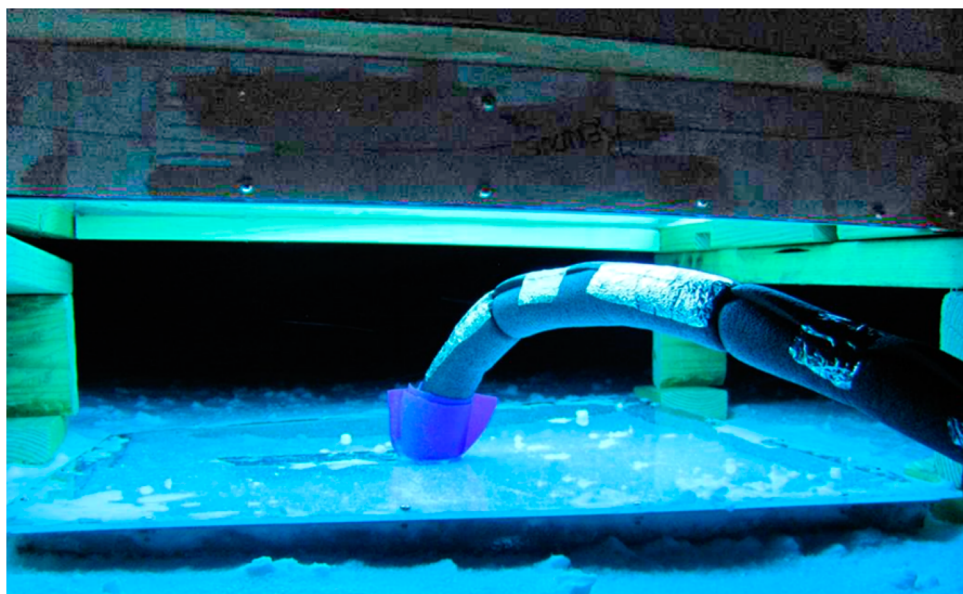


**Figure 1.** Image of the illuminated in-snowpack sampling setup for an experiment conducted on Feb 11, 2014, showing the lamps suspended above the snowpack with an insulated sample line passing through the snow cover and into the snow sampling hole.

amu) showed a slope of  $1.201 \pm 0.004$  ( $R^2 = 0.991$ ), confirming the presence of one Cl and one Br atom (Figure S3 of the Supporting Information, with an isotopic ratio of 1.3).

**2.2. Snowpack Interstitial Air Experiments.** In-snowpack experiments were performed during early morning or late evening in the absence of natural ultraviolet (UV) radiation to allow control for when and how long the snowpack was irradiated. A 380 cm fluorinated ethylene propylene (FEP) line (1.27 cm inner diameter) heated to 30 °C was attached to the CIMS inlet to allow for sampling of the snowpack interstitial air. Br<sub>2</sub> and Cl<sub>2</sub> line loss tests were performed, showing average losses of ~7 and ~3.5%, respectively. Lab studies have shown that HOBr adsorbed onto Teflon surfaces can be converted to Br<sub>2</sub>.<sup>23</sup> As a preventative measure, we cleaned our sample line before and after every experiment by rinsing with Milli-Q water and drying with N<sub>2</sub>. Control experiments were performed during which the CIMS inlet was switched between the experiment sampling line and an inlet described by Liao et al.<sup>22</sup> that was designed to minimize inlet losses and previously compared to differential optical absorption spectroscopy measurements of BrO. For these experiments, both inlets were placed at the same height above the snowpack. A paired *t* test showed that there was no significant difference (95% confidence interval) between Br<sub>2</sub> (and Cl<sub>2</sub>) mole ratios measured by the two inlets, suggesting that the cleaned sampling line used herein did not impact the molecular halogen mole ratios beyond their measurement uncertainties.

To ensure that ambient air was not directly sampled during in-snowpack sampling, a custom snow cover was built using a 61 × 61 cm piece of 0.6 cm thick Acrylite OP-4 (CRYO Industries) mounted to an aluminum frame with a 7.6 cm edge to press into the snowpack. The snow cover provides ~67% transmission of 280 nm radiation, rising to ~78% at 300 nm and ~92% at 400 nm. A 5.4 cm inner diameter circle was cut out of the center of the cover for the sample line. Before in-snow experiments, the snow cover was pushed into the snowpack until the Acrylite sheet contacted the snowpack surface. A sampling hole of a desired depth was then bored into the snowpack using a clean stainless-steel ice auger drill bit,

leaving a 5.4 cm inner diameter hole into which the sample line was inserted, and then sealed to the cover. To irradiate the snowpack, six solar simulating lights (UVA-340, Q-Lab, 300–400 nm with a maximum wattage at 340 nm) housed in a wooden box were placed 15 cm above the snow cover. For the Feb 11 in-snow experiment, ozone was pumped into the snowpack via a line alongside the sampling line. The ozone was generated by passing breathing quality compressed air (1.5 lpm) through an O<sub>3</sub> generator (model 97-0067-01, UVP). An image from the Feb 11 in-snowpack experiment setup is shown in Figure 1.

**2.3. Vertical Profile and Flux Experiments.** Vertical profile measurements of molecular halogens (Br<sub>2</sub> and Cl<sub>2</sub>) were achieved by sampling ambient air at various heights (0–100 cm) above the tundra snowpack in the same location as the snowpack interstitial air experiments. The 380 cm FEP line (1.27 cm inner diameter, as described in section 2.2) heated to 30 °C was attached to an adjustable bipod that allowed for consistent height variations above the snowpack.

Flux values were calculated using the gradient method equation (eq 1) described by Guimbaud et al.<sup>24</sup>

$$\text{flux} = -K \frac{dC}{dz} \quad (1)$$

where dC/dz is the change in concentration (C) as a function of height above the snowpack surface, approximated by  $C(z_2) - C(z_1)/(z_2 - z_1)$ , where *z* is the measurement height (m). The eddy diffusivity (K) was calculated using eq 2.

$$K = \kappa z_s u^* \quad (2)$$

For eq 2, *u*\* represents the friction velocity,  $\kappa$  is the van Karman constant (0.4), and *z*<sub>s</sub> is the logarithmic mean sampling height. The friction velocity was calculated, using eq 3, where *U* is the mean measured wind speed (m/s) at 10 m (section 2.1) and *z*<sub>0</sub> is the roughness length (m).<sup>25</sup>

$$u^* = \frac{\kappa U(10 \text{ m})}{\ln\left(\frac{10 \text{ m}}{z_0}\right)} \quad (3)$$

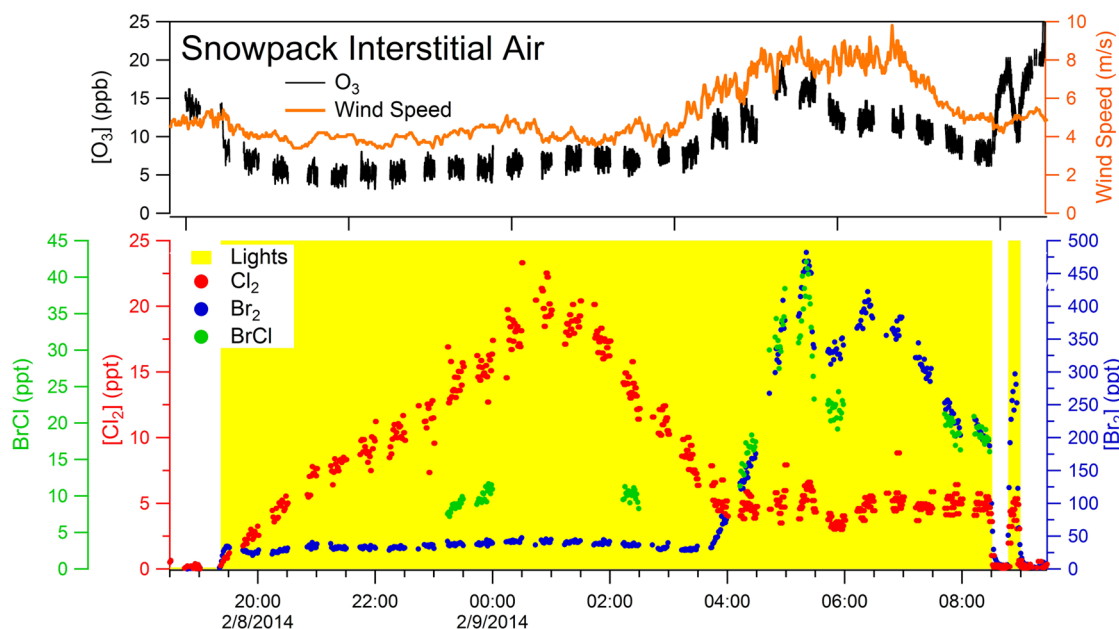


**Figure 2.** (Top) Snowpack interstitial air  $O_3$  and (bottom) molecular halogen mole ratios (1 min averaging) at a snow depth of 10 cm during the Feb 8–9, 2014 snowpack artificial irradiation experiment. The yellow-shaded period indicates the time period of artificial irradiation. The wind speed at 10 m above the snowpack is provided as a comparison. Regular data gaps correspond to times of background measurements and calibrations. BrCl data are only shown for time periods when the signals corresponded to the proper BrCl isotope ratio; prolonged BrCl data gaps correspond to times when there was evidence of an interference.

The logarithmic mean for the two sampling heights ( $z_s$ ) was calculated using eq 4, where  $z_1$  represents the lower sampling height and  $z_2$  represents the upper sampling height of CIMS.

$$z_s = \frac{z_2 - z_1}{\ln\left(\frac{z_2}{z_1}\right)} \quad (4)$$

The logarithmic mean of the two sampling heights, the friction velocity, and the van Karman constant were combined to calculate the eddy diffusivity values for each sampling segment.  $u^*$  is the only changing component of the eddy diffusivity, because it depends upon the wind speed, which is generally changing throughout the experiments. A comparison of wind speeds at the study field site and the NOAA Barrow Observatory in March 2012<sup>26</sup> showed that winds at the observatory were  $25 \pm 27\%$  faster than at the study field site, separated only by flat tundra; therefore, a wind speed uncertainty of  $\pm 27\%$  is considered in the calculated flux uncertainty. The average roughness length of  $0.000\ 19 \pm 0.000\ 01$  m, measured near Utqiagvik and described in the Supporting Information,<sup>27</sup> is used in the eddy diffusivity calculation.

### 3. RESULTS AND DISCUSSION

**3.1. Snowpack Interstitial Air Experiments.** To examine the production of molecular halogens via snowpack reactions, two snowpack experiments were conducted in Feb 2014, during early morning/late evening, so that the snowpack exposure to UV radiation could be controlled through the use of lamps. The experiment conducted on Feb 8 started at 18:30 [Alaska Standard Time (AKST)], 2 h after the sun had set for the day. In the absence of light, the  $Br_2$  and  $Cl_2$  signals, within the snowpack interstitial air, were below the CIMS LODs of 3.6 and 1.0 ppt, respectively (Figure 2). This indicates the lack of or minor contribution by a dark production mechanism. To

examine the photochemical nature of molecular halogen production, the snowpack was then artificially irradiated from Feb 8 at 19:30 to Feb 9 at 20:30. The ambient temperature ranged from 255 to 259 K through this period. During snowpack illumination,  $Br_2$ ,  $Cl_2$ , and  $BrCl$  were observed and the mole ratios of these molecular halogens quickly approached zero upon removal of the simulated solar radiation (Figure 2). This suggests a photochemical production mechanism for  $Br_2$ ,  $Cl_2$ , and  $BrCl$ , as shown previously for  $Br_2$  in the ambient snowpack<sup>12</sup> and using artificial saline snow and ice in the laboratory.<sup>28,29</sup> Interstitial air  $O_3$  levels showed an opposite trend compared to the molecular halogens (Figure 2), showing evidence of halogen-mediated ozone destruction.<sup>30</sup>

During the Feb 8–9 experiment,  $Cl_2$  production followed a different pattern compared to  $Br_2$  and  $BrCl$ . Both  $Br_2$  and  $Cl_2$  showed immediate production upon snowpack illumination (Figure 2). At this time, the signals of the  $BrCl$  masses did not align with the proper isotope ratio, showing a significant interference and suggesting a lack of  $BrCl$  present. After 30 min,  $Br_2$  reached a constant mole ratio ( $\sim 40$  ppt), in contrast to  $Cl_2$ , which instead slowly rose for  $\sim 5$  h from 0 to 20 ppt, during which time  $BrCl$  was also observed at  $\sim 10$  ppt (Figure 2). Once  $Cl_2$  reached its maximum mole ratio during the artificial irradiation of the snowpack on Feb 9, it slowly decreased until  $\sim 4:00$  (AKST), when the  $Cl_2$  level plateaued (Figure 2). Also, at  $\sim 4:00$ , an increase in wind speed from 4 to  $8\ m\ s^{-1}$  occurred. Wind motion on the windward side of surface features (e.g., sastrugi) causes a pressure increase/decrease on the windward/leeward side of the bumps. This forces ambient air into the snowpack, which mixes and pushes interstitial air out of the snowpack (wind pumping),<sup>31</sup> and has been shown to modulate interstitial air ozone concentrations.<sup>30</sup> The observed wind speed increase led to an observed rise in the snowpack interstitial air  $O_3$  concentration from 7 to 17 ppb, with concurrent increases in  $Br_2$  and  $BrCl$  to  $\sim 475$  and 42 ppt,

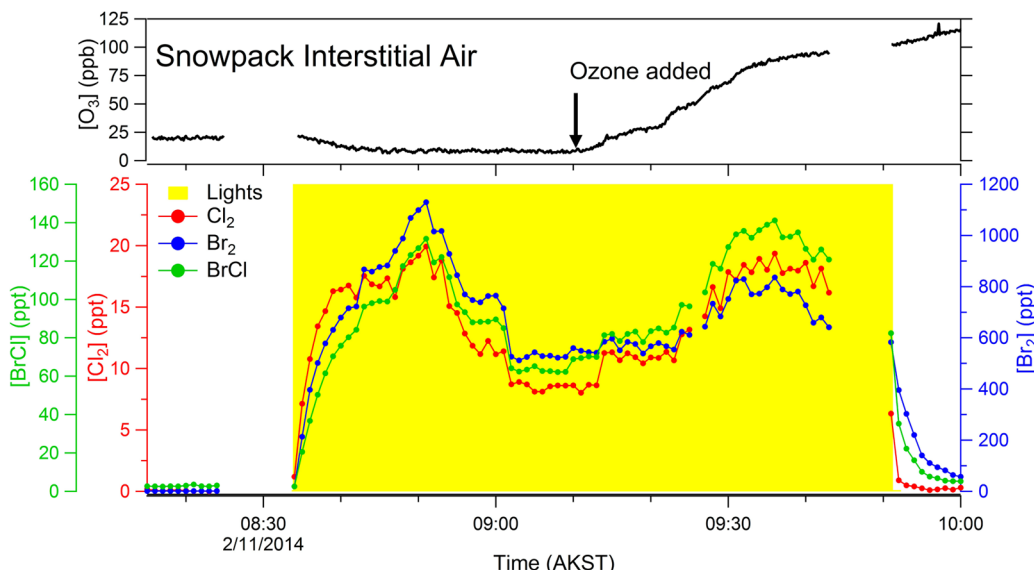
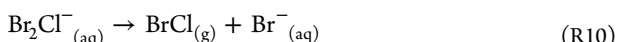
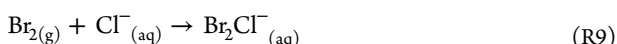


**Figure 3.** (Top) Snowpack interstitial air  $O_3$  and (bottom) molecular halogen mole ratios (1 min averaging) at a snow depth of 10 cm during the Feb 11, 2014 snowpack artificial irradiation experiment. The yellow-shaded period indicates the time period of artificial irradiation. Data gaps correspond to times of background measurements and calibrations.

respectively (corresponding to increases by factors of 12 and 4, respectively) (Figure 2). The enhanced  $Br_2$  and  $BrCl$  production is consistent with an interstitial air bromine explosion, as previously observed for ozone-enhanced photochemical production of  $Br_2$  from the Arctic surface snowpack during snow chamber experiments.<sup>12</sup> This involves the snowpack interstitial air production and heterogeneous reaction of HOX and/or XONO<sub>2</sub> to release X<sub>2</sub>/XY (reactions R1–R8). Similar to the recycling reaction of HOBr with Br<sup>−</sup> to produce  $Br_2$  (reaction R7), previous laboratory studies have shown the production of  $BrCl$  from the reaction of HOBr with Cl<sup>−</sup><sup>32–34</sup> or from interhalogen reactions, such as reactions R9 and R10.<sup>35</sup>



It is clear that the molecular halogens were produced within the snowpack rather than transported from the overlying air, because the mole ratios rapidly dropped below LODs (and  $O_3$  increased) when the snowpack was no longer irradiated [at 8:30 and 9:00 (AKST); Figure 2]. In contrast to  $Br_2$  and  $BrCl$ , there was no clear impact of  $O_3$  on  $Cl_2$  production, with the  $Cl_2$  mole ratio near constant at 5 ppt during this period (Figure 2).

To further investigate the role of ozone in molecular halogen production, a second in-snowpack experiment was conducted on the morning of Feb 11, 2014 prior to sunrise (Figure 3). As in the Feb 8–9 experiment, all three molecular halogens were below the CIMS LOD during dark sampling at the beginning of the experiment. Upon illumination,  $Br_2$ ,  $Cl_2$ , and  $BrCl$  production instantly occurred. The snowpack interstitial air  $O_3$  concentration was initially ~25 ppb (as compared to 5–18 ppb on Feb 8–9), resulting in higher  $Br_2$  and  $BrCl$  concentrations (maxima of 1100 and 140 ppt, respectively; Figure 3) than those observed during the Feb 8–9 experiment (Figure 2). This is consistent with a strong interstitial air bromine explosion. However, unlike during the previous experiment, the production of all three molecular halogens reached a maximum more quickly (after ~15 min), after which the concentrations decreased and leveled off after ~30 min of

irradiation (Figure 3). The decrease in molecular halogen levels coincided with decreased  $O_3$  levels as a result of the reaction with bromine atoms produced from photolysis of  $Br_2$  and  $BrCl$ . Therefore, the ozone destruction seems to slow the bromine explosion cycle, thereby reducing molecular halogen production. At 9:10 (AKST) on Feb 11, externally generated  $O_3$  was pumped into the snowpack at a distance of 5 cm horizontally away from the sampling location. As the ozone level in the snowpack interstitial air increased from 8 to 100 ppb, the snowpack  $BrCl$  and  $Cl_2$  mole ratios more than doubled, with  $Br_2$  increasing by ~60% (Figure 3), showing that the production of all three molecular halogens was enhanced with significant  $O_3$  addition, likely through the halogen explosion cycle (reactions R2–R8). However, again, a maximum was reached at 9:35 (AKST), such that the levels of the molecular halogens decreased some, even with additional  $O_3$  at this point (Figure 3). When the lamps were switched off, all of the molecular halogens decayed rapidly, consistent with a photochemical production mechanism (Figure 3).

During both in-snowpack experiments,  $Br_2$  mole ratios were higher than  $BrCl$  (by factors of 4–11) and  $Cl_2$  (by factors of 2–95). Bromide is expected to be enriched at the disordered interface of the snow grain surface.<sup>36–40</sup> A photochemical hydroxyl radical (OH)-mediated production mechanism based on previous laboratory studies<sup>28</sup> was suggested for the production of  $Br_2$  from the Arctic surface snow.<sup>12</sup> In addition to the surface enrichment, bromide has a greater aqueous-phase reaction rate constant with OH compared to chloride, leading to preferential oxidation of bromide.<sup>28</sup> At Utqiagvik, snow OH has been shown to be produced through photolysis of H<sub>2</sub>O<sub>2</sub>, nitrite, and nitrate.<sup>41</sup> The observed dominance of  $Br_2$  is consistent with laboratory measurements of OH oxidation of frozen NaCl/NaBr mixtures with Cl<sup>−</sup>/Br<sup>−</sup> seawater ratios, showing a  $BrCl$  yield at 3% of the  $Br_2$  yield, with no  $Cl_2$  measured above the method detection limit for frozen seawater at pH 7, with a lower  $BrCl$  yield (2%) at pH 2.<sup>42</sup> In comparison, the measurements described herein show greater relative fractions of  $BrCl$  and the presence of  $Cl_2$ , the latter of which may be due to the lower LOD of the instrument used herein.

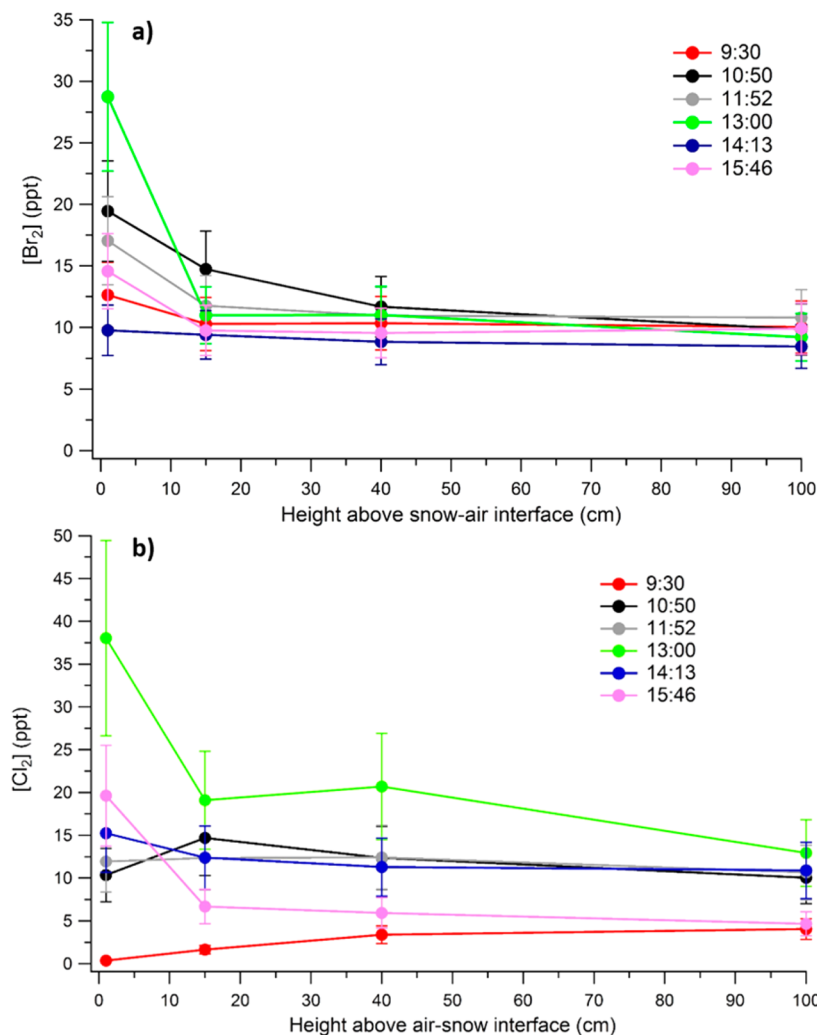


**Figure 4.** (a) Br<sub>2</sub> and (b) Cl<sub>2</sub> vertical profile measurements on Feb 16, 2014 with the time (AKST) denoting the start of the vertical profile conducted at the height closest to the snow surface.

The greater relative abundance of BrCl and Cl<sub>2</sub> herein than predicted from previous laboratory studies may be due to their greater photolysis rates compared to Br<sub>2</sub> (by factors of 2.3 and 1.7, respectively) for the lamps used (maximum radiation at 340 nm), thereby promoting heterogeneous recycling and increasing molecular halogen production compared to solar radiation conditions, where Br<sub>2</sub> photolysis is relatively faster.<sup>43</sup> This is also consistent with the observed magnitude of the increases in Br<sub>2</sub> (1.5×), BrCl (2.2×), and Cl<sub>2</sub> (2.6×) mole ratios from 8 to 100 ppb O<sub>3</sub> during the Feb 11 experiment.

When comparing the Feb 8–9 and Feb 11 experiments under <10 ppb O<sub>3</sub> conditions, Br<sub>2</sub> and BrCl mole ratios were higher on Feb 11 by factors of 14 and 7. Similar to the case for Br<sub>2</sub>, Sjostedt and Abbott<sup>42</sup> previously proposed that BrCl could form in the condensed phase following OH oxidation of bromide and/or chloride. In addition to undergoing photolysis (reaction R1), BrCl can also react with Br<sup>−</sup> to produce Br<sub>2</sub>.<sup>33</sup> While the snow temperature was not measured herein, the air temperature during the experiments ranged from 255 to 259 K on Feb 8–9 and was 247 K on Feb 11. While the air temperatures on both days were above the eutectic point for the formation of NaBr·2H<sub>2</sub>O (245 K), the snow temperature on Feb 11 was likely below the eutectic point for the formation of NaCl·2H<sub>2</sub>O (251 K).<sup>44</sup> Limited Cl<sup>−</sup> available for reaction

with the condensed phase oxidant enhances the relative abundance of Br<sup>−</sup> available for oxidation, likely leading to the increased Br<sub>2</sub> and BrCl production<sup>42</sup> observed on Feb 11. For context, the bulk snow meltwater pH (5.3–5.8), [Br<sup>−</sup>] (0.2–0.4 μM), and [Cl<sup>−</sup>] (0.4–0.6 mM) were similar for samples collected Feb 5, 23, and 28, 2014 (Table S1 of the Supporting Information), suggesting that overall snow pH and Br<sup>−</sup>/Cl<sup>−</sup> ratios were unlikely to drive the differences in molecular halogen production.

In contrast to the Br<sub>2</sub> and BrCl trends observed, Cl<sub>2</sub> mole ratios were greater by a factor of 3 on Feb 8–9 (20 ppt) compared to Feb 11 (7 ppt), under <10 ppb O<sub>3</sub> conditions. On Feb 11, Cl<sub>2</sub> production was likely limited by available Cl<sup>−</sup>, because the snow temperature was likely below the eutectic point for the formation of NaCl·2H<sub>2</sub>O (251 K).<sup>44</sup> In their study of the heterogeneous OH reaction with frozen saline solutions at 248 K, Sjostedt and Abbott<sup>42</sup> suggested that the lack of observed Cl<sub>2</sub> production was due to limited Cl<sup>−</sup> available for reaction as a result of NaCl·2H<sub>2</sub>O precipitation. Similarly, Wren et al.<sup>29</sup> observed decreased photochemical Cl<sub>2</sub> production below 252 K from artificial saline snow. Overall, maximum Cl<sub>2</sub> mole ratios were similar between the Feb 8–9 and Feb 11 experiments (~20 ppt), with increased Cl<sub>2</sub> observed for increased O<sub>3</sub> on Feb 11 only, perhaps as a result of differences

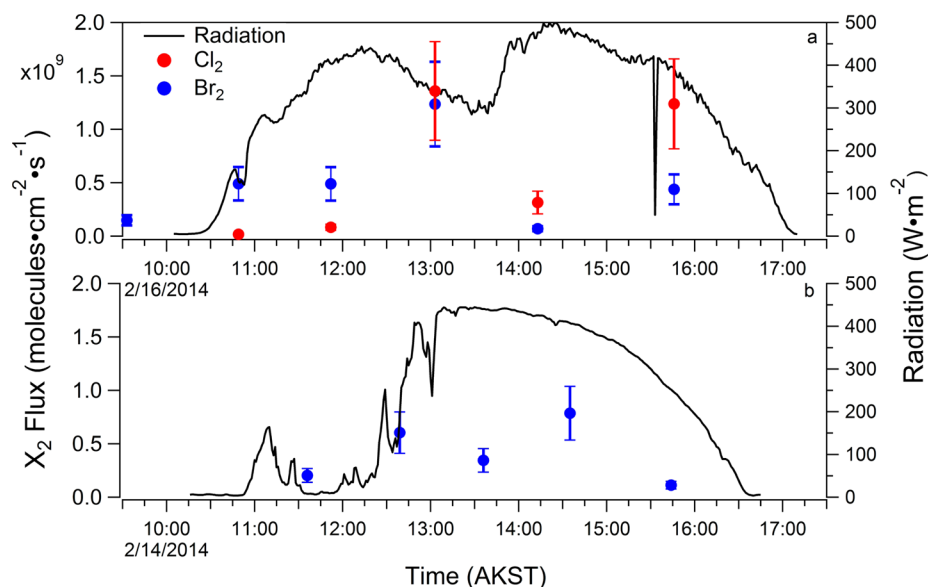


**Figure 5.** Snowpack  $\text{Br}_2$  and  $\text{Cl}_2$  fluxes (also in Table 1) calculated from gradient profiles (Figure 4) with corresponding radiation on (top) Feb 16, 2014 and (bottom) Feb 14, 2014.  $\text{Cl}_2$  mole ratios were below the CIMS LOD on Feb 14.

**Table 1. Calculated Snowpack Fluxes Based on ~1 h Vertical Gradient Measurements (Figure 4) for  $\text{Br}_2$  and  $\text{Cl}_2$  on Feb 14 and 16, 2014, and Average Solar Radiation during Each Measurement Period<sup>a</sup>**

time (AKST)	$\text{Br}_2$ flux (molecules $\text{cm}^{-2} \text{s}^{-1}$ )	$\text{Cl}_2$ flux (molecules $\text{cm}^{-2} \text{s}^{-1}$ )	solar radiation ( $\text{W m}^{-2}$ )
Feb 14, 2014, 11:36	$2.0 (\pm 0.6) \times 10^8$	N/A	10
Feb 14, 2014, 12:39	$6. (\pm 2) \times 10^8$	N/A	191
Feb 14, 2014, 13:36	$4. (\pm 1) \times 10^8$	N/A	440
Feb 14, 2014, 14:35	$8. (\pm 2) \times 10^8$	N/A	405
Feb 14, 2014, 15:44	$1.1 (\pm 0.3) \times 10^8$	N/A	248
Feb 16, 2014, 09:33	$1.5 (\pm 0.5) \times 10^8$	N/A	N/A
Feb 16, 2014, 10:49	$5. (\pm 2) \times 10^8$	$0.16 (\pm 0.05) \times 10^8$	125
Feb 16, 2014, 11:52	$5. (\pm 2) \times 10^8$	$0.8 (\pm 0.3) \times 10^8$	403
Feb 16, 2014, 13:03	$12. (\pm 4) \times 10^8$	$14. (\pm 4) \times 10^8$	331
Feb 16, 2014, 14:13	$0.7 (\pm 0.2) \times 10^8$	$3. (\pm 1) \times 10^8$	463
Feb 16, 2014, 15:46	$4. (\pm 1) \times 10^8$	$12. (\pm 4) \times 10^8$	383

<sup>a</sup>Note that  $\text{Cl}_2$  mole ratios were below the CIMS LOD on Feb 14.

in the production of  $\text{HO}_2$  and/or  $\text{NO}_2$ . Knipping et al.<sup>45</sup> provided support for an OH-facilitated mechanism for the production of  $\text{Cl}_2$  by observing the release of  $\text{Cl}_2$  from irradiated aqueous  $\text{NaCl}$  aerosols in the presence of ozone. However, Wren et al.<sup>29</sup> concluded that initial  $\text{Cl}_2$  production resulted from photolysis of  $\text{BrCl}$  to produce  $\text{HOCl}$ , which reacted with  $\text{Cl}^-$  to produce  $\text{Cl}_2$  (reactions R1–R4, R7, and R8). Analogous reactions R1, R2, and R5–R8, involving production of  $\text{ClONO}_2$  and subsequent reaction with  $\text{Cl}^-$ , can also produce  $\text{Cl}_2$ .<sup>46</sup> During elevated ozone (>10 ppb) periods of the two experiments,  $\text{BrCl}$  mole ratios were factors of 7–8 greater than  $\text{Cl}_2$  mole ratios.

**3.2. Vertical Profile Experiments.** To examine above snowpack concentration gradients and calculate fluxes of the molecular halogens, vertical profile experiments were conducted on Feb 14 and 16, 2014 from 0 to 100 cm above the snowpack. For both experiments, ambient air was sampled from ~9:00 to 16:00 (AKST) to allow for a complete diurnal radiation cycle to be examined, given the photochemical production of the molecular halogens, as discussed in the previous section. Both experiments yielded increasing mole ratio gradients of  $\text{Br}_2$  and  $\text{Cl}_2$  near the snow surface at mid-day (Figure 4 and Figure S4 of the Supporting Information),

consistent with in-snowpack production and emission to the overlying atmosphere. We could not quantify  $\text{BrCl}$  as a result of an ambient air interference. During peak sunlight [ $\sim 13:00$  (AKST)], the greatest  $\text{Br}_2$  and  $\text{Cl}_2$  concentrations were observed compared to hours of reduced sunlight [9:30 and 15:46 (AKST)], consistent with radiation-dependent production.

The concentration gradients were combined with calculated eddy diffusivity values to determine time varying flux values for  $\text{Br}_2$  and  $\text{Cl}_2$ , as shown in Figure 5 and Table 1. To date, only the  $\text{Br}_2$  fluxes necessary to simulate observed  $\text{BrO}$  have been reported in the literature, because the majority of the Arctic-based halogen observations have been with respect to  $\text{BrO}$ , for which measurements have existed for a couple of decades.<sup>47</sup> These modeling studies<sup>9,10,48,49</sup> have estimated  $\text{Br}_2$  fluxes from  $9.0 \times 10^7$  to  $2.7 \times 10^9$  molecules  $\text{cm}^{-2} \text{s}^{-1}$  for springtime Arctic halogen chemistry. Our observed  $\text{Br}_2$  fluxes presented here ( $0.7$ – $12 \times 10^8$  molecules  $\text{cm}^{-2} \text{s}^{-1}$ ) encompass a very similar range of fluxes as for the modeling studies. A significant difference between our flux values and those reported from modeling studies is that our flux values are based on observations from mid-February when ozone depletion has not yet occurred (atmospheric  $\text{O}_3$  of ~35 ppb during the Jan–

Feb study). In contrast, modeling studies are typically based on springtime ozone depletion conditions, when solar irradiance and halogen concentrations are greater.<sup>13</sup> Coincident with increasing snowpack sunlight absorption,<sup>50</sup> France et al.<sup>41</sup> observed increasing condensed-phase OH production from the photolysis of  $\text{NO}_2^-$ ,  $\text{NO}_3^-$ , and  $\text{H}_2\text{O}_2$  through March 2009 near Utqiagvik. If the molecular halogen production is limited by condensed phase oxidant production, this would increase molecular halogen production.<sup>28</sup> At the same time, during the ODEs, the production of gas-phase HBr, HCl, HOBr, and HOCl deposit onto the surface snowpack, altering snowpack  $[\text{Br}^-]$  and  $[\text{Cl}^-]$  and resulting halogen production.<sup>11</sup> On the basis of these factors, we can assume that our flux values likely represent a less active snowpack compared to later in the spring when the additional radiation prompts ODEs that promote chemistry, which likely leads to a higher flux rate of molecular halogens from the snowpack. This is also supported when comparing our observed  $\text{Br}_2$  and  $\text{Cl}_2$  ambient concentrations in February to those observed during March/April. In this study,  $\text{Br}_2$  and  $\text{Cl}_2$  daytime above-snowpack concentrations ranged from 5 to 25 ppt and from 5 to 20 ppt, respectively, while previous observations in mid to late March at Utqiagvik showed  $\text{Br}_2$  ranging from 0 to 5 ppt and  $\text{Cl}_2$  ranging from 10 to 400 ppt during the day.<sup>15–17</sup> However, it should be noted that the measured atmospheric concentrations of molecular halogens depend upon several variables, including emission rates, atmospheric mixing, recycling, and photochemical loss. During the spring months of April and March, both atmospheric mixing and photochemical loss of molecular halogens will be greater compared to February. This further supports the suggestion that the emission rates of molecular halogens from the snowpack are likely to be greater in the spring compared to our winter time observations.

#### 4. CONCLUSION

From in-snowpack measurements conducted in the coastal Arctic (Utqiagvik, AK) in Feb 2014, the surface snowpack was shown to be a significant source of atmospheric  $\text{Br}_2$ ,  $\text{BrCl}$ , and  $\text{Cl}_2$ . Prior to this work, the sources and production pathways of Arctic atmospheric  $\text{Cl}_2$  and  $\text{BrCl}$  were unknown. This is important because the Arctic is currently undergoing rapid sea ice transformation and loss, providing urgency to gain the knowledge to properly simulate future atmospheric composition. The observed snowpack production of  $\text{Cl}_2$  and  $\text{BrCl}$  is particularly important to the photolytic production of Cl atoms, which are highly reactive toward hydrocarbons, including the greenhouse gas methane.<sup>19,51</sup> From vertical profile experiments, flux values for  $\text{Cl}_2$  and  $\text{Br}_2$  were derived for the tundra snowpack. Using the calculated flux values, we were able to evaluate the snow as an overall source of atmospheric molecular halogens and found it to have the potential to be a dominant source. These empirically derived  $\text{Br}_2$  and  $\text{Cl}_2$  snowpack fluxes should be incorporated into models to evaluate the importance of the snowpack as a molecular halogen source and to advance our understanding of Arctic atmospheric composition.

Notably, molecular halogen production was observed upon artificial illumination of the snowpack immediately following polar sunrise and before an ODE was observed in the lower troposphere.  $\text{Br}_2$  and  $\text{BrCl}$  production were consistent with condensed-phase photochemical oxidation occurring at the snow grain surface, with enhanced production in the presence of ozone as a result of heterogeneous recycling within the snowpack intersstitial air. Decreased production of  $\text{Cl}_2$  and

increased production of  $\text{Br}_2$  and  $\text{BrCl}$  were observed during an in-snowpack experiment at air temperatures below the eutectic point for the formation of  $\text{NaCl}\cdot 2\text{H}_2\text{O}$ , whereas increased  $\text{Cl}_2$  and decreased  $\text{Br}_2$  and  $\text{BrCl}$  production were observed above this eutectic point as a result of greater chloride availability and competition for a photochemically produced condensed-phase oxidant, such as the hydroxyl radical. Future work should pursue physical and chemical characterization of the snow grain surface to provide additional insights into the most important photochemical mechanisms and controlling factors in snowpack molecular halogen production.<sup>11</sup>

#### ■ ASSOCIATED CONTENT

##### S Supporting Information

The Supporting Information is available free of charge on the ACS Publications website at DOI: [10.1021/acsearthspacechem.7b00014](https://doi.org/10.1021/acsearthspacechem.7b00014).

Description of snow collection and measurements, as well as the roughness length calculation, isotopic ratio plots for  $\text{Br}_2$ ,  $\text{Cl}_2$ , and  $\text{BrCl}$  during an in-snowpack experiment on Feb 11, 2014 (Figures S1–S3),  $\text{Br}_2$  above-snowpack vertical profile data from Feb 14, 2014 (Figure S4), and pH and inorganic ion concentrations of melted surface snow on Feb 5, 23, and 28, 2014 (Table S1) ([PDF](#))

#### ■ AUTHOR INFORMATION

##### Corresponding Author

\*E-mail: [prattka@umich.edu](mailto:prattka@umich.edu).

##### ORCID

K. A. Pratt: 0000-0003-4707-2290

##### Notes

The authors declare no competing financial interest.

#### ■ ACKNOWLEDGMENTS

The authors gratefully acknowledge support from the National Science Foundation (NSF, ARC-1107695 and PLR-1417668). UMIAQ and Polarfield Services are thanked for Utqiagvik logistics assistance. Wind and temperature data were obtained from the National Oceanic and Atmospheric Administration (NOAA) Barrow Observatory. Radiation data were obtained from the Atmospheric Radiation Measurement (ARM) program sponsored by the Climate and Environmental Sciences Division, Office of Biological and Environmental Research, Office of Science, United States Department of Energy. Ignatius Rigor (University of Washington) is thanked for 2012 wind speed data. Nathaniel May (University of Michigan) is thanked for assistance with surface snow measurements, and Siyuan Wang (University of Michigan) is thanked for discussions. Molecular halogen vertical profile data are available through the NSF Arctic Data Center.

#### ■ REFERENCES

- (1) Simpson, W. R.; von Glasow, R.; Riedel, K.; Anderson, P. S.; Ariya, P.; Bottenheim, J. W.; Burrows, J. P.; Carpenter, L. J.; Frieß, U.; Goodsite, M.; Heard, D. E.; Hutterli, M. A.; Jacobi, H.-W.; Kaleschke, L.; Neff, B.; Plane, J. M. C.; Platt, U.; Richter, A.; Roscoe, H. K.; Sander, R.; Shepson, P. B.; Sodeau, J.; Steffen, A.; Wagner, T.; Wolff, E. W. Halogens and Their Role in Polar Boundary-Layer Ozone Depletion. *Atmos. Chem. Phys.* 2007, 7, 4375–4418.
- (2) Abbatt, J. P. D.; Thomas, J. L.; Abrahamsson, K.; Boxe, C. S.; Granfors, A.; Jones, A. E.; King, M. D.; Saiz-Lopez, A.; Shepson, P. B.;

Sodeau, J.; Toohey, D. W.; Toubin, C.; von Glasow, R.; Wren, S. N.; Yang, X. Halogen Activation via Interactions with Environmental Ice and Snow in the Polar Lower Troposphere and Other Regions. *Atmos. Chem. Phys.* **2012**, *12*, 6237–6271.

(3) Barrie, L. A.; Bottenheim, J. W.; Schnell, R. C.; Crutzen, P. J.; Rasmussen, R. A. Ozone Destruction and Photochemical Reactions at Polar Sunrise in the Lower Arctic Atmosphere. *Nature* **1988**, *334*, 138–141.

(4) Oltmans, S. J.; Schnell, R. C.; Sheridan, P. J.; Peterson, R. E.; Li, S.-M.; Winchester, J. W.; Tans, P. P.; Sturges, W. T.; Kahl, J. D.; Barrie, L. A. Seasonal Surface Ozone and Filterable Bromine Relationship in the High Arctic. *Atmos. Environ.* **1989**, *23* (11), 2431–2441.

(5) Oltmans, S. J.; Johnson, B. J.; Harris, J. M. Springtime Boundary Layer Ozone Depletion at Barrow, Alaska: Meteorological Influence, Year-to-Year Variation, and Long-Term Change. *J. Geophys. Res.: Atmos.* **2012**, *117* (D14), 2156–2202.

(6) McConnell, J. C.; Henderson, G. S.; Barrie, L. A.; Bottenheim, J. W.; Niki, H.; Langford, C. H.; Templeton, E. M. J. Photochemical Bromine Production Implicated in Arctic Boundary-Layer Ozone Depletion. *Nature* **1992**, *355*, 150–152.

(7) Fan, S.-M.; Jacob, D. J. Surface Ozone Depletion in the Arctic Spring Sustained by Bromine Reactions on Aerosols. *Nature* **1992**, *359* (6395), 522–524.

(8) Michalowski, B. A.; Francisco, J. S.; Li, S. M.; Barrie, L. A.; Bottenheim, J. W.; Shepson, P. B. A Computer Model Study of Multiphase Chemistry in the Arctic Boundary Layer during Polar Sunrise. *J. Geophys. Res.: Atmos.* **2000**, *105* (D12), 15131–15145.

(9) Lehrer, E.; Hönniger, G.; Platt, U. A One Dimensional Model Study of the Mechanism of Halogen Liberation and Vertical Transport in the Polar Troposphere. *Atmos. Chem. Phys.* **2004**, *4*, 2427–2440.

(10) Piot, M.; von Glasow, R. The Potential Importance of Frost Flowers, Recycling on Snow, and Open Leads for Ozone Depletion Events. *Atmos. Chem. Phys.* **2008**, *8*, 2437–2467.

(11) Simpson, W. R.; Alvarez-aviles, L.; Douglas, T. A.; Sturm, M.; Domine, F. Halogens in the Coastal Snow Pack near Barrow, Alaska: Evidence for Active Bromine Air-Snow Chemistry during Springtime. *Geophys. Res. Lett.* **2005**, *32*, 2–5.

(12) Pratt, K. A.; Custard, K. D.; Shepson, P. B.; Douglas, T.; Pöhler, D.; General, S.; Zielcke, J.; Simpson, W. R.; Platt, U.; Tanner, D. J.; Huey, L. G.; Carlsen, M.; Stirm, B. H. Photochemical Production of Molecular Bromine in Arctic Surface Snowpacks. *Nat. Geosci.* **2013**, *6* (5), 351–356.

(13) Foster, K. L.; Plastridge, R. A.; Bottenheim, J. W.; Shepson, P. B.; Finlayson-Pitts, B. J.; Spicer, C. W. The Role of Br<sub>2</sub> and BrCl in Surface Ozone Destruction at Polar Sunrise. *Science (Washington, DC, U. S.)* **2001**, *291* (5503), 471–474.

(14) Spicer, C. W.; Plastridge, R. A.; Foster, K. L.; Finlayson-Pitts, B. J.; Bottenheim, J. W.; Grannas, A. M.; Shepson, P. B. Molecular Halogens before and during Ozone Depletion Events in the Arctic at Polar Sunrise: Concentrations and Sources. *Atmos. Environ.* **2002**, *36*, 2721–2731.

(15) Liao, J.; Huey, L. G.; Tanner, D. J.; Flocke, F. M.; Orlando, J. J.; Neuman, J. A.; Nowak, J. B.; Weinheimer, A. J.; Hall, S. R.; Smith, J. N.; Fried, A.; Staebler, R. M.; Wang, Y.; Koo, J.-H.; Cantrell, C. A.; Weibring, P.; Walega, J.; Knapp, D. J.; Shepson, P. B.; Stephens, C. R. Observations of Inorganic Bromine (HOBr, BrO, and Br<sub>2</sub>) Speciation at Barrow, Alaska, in Spring 2009. *J. Geophys. Res.* **2012**, *117* (D14), D00R16.

(16) Liao, J.; Huey, L. G.; Liu, Z.; Tanner, D. J.; Cantrell, C. a.; Orlando, J. J.; Flocke, F. M.; Shepson, P. B.; Weinheimer, A. J.; Hall, S. R.; Ullmann, K.; Beine, H. J.; Wang, Y.; Ingall, E. D.; Stephens, C. R.; Hornbrook, R. S.; Apel, E. C.; Riemer, D.; Fried, A.; Mauldin, R. L.; Smith, J. N.; Staebler, R. M.; Neuman, J. A.; Nowak, J. B. High Levels of Molecular Chlorine in the Arctic Atmosphere. *Nat. Geosci.* **2014**, *7* (2), 91–94.

(17) Custard, K. D.; Pratt, K. A.; Wang, S.; Shepson, P. B. Constraints on Arctic Atmospheric Chlorine Production through Measurements and Simulations of Cl<sub>2</sub> and ClO. *Environ. Sci. Technol.* **2016**, *50* (22), 12394–12400.

(18) Saiz-Lopez, A.; von Glasow, R. Reactive Halogen Chemistry in the Troposphere. *Chem. Soc. Rev.* **2012**, *41* (19), 6448–6472.

(19) Simpson, W. R.; Brown, S. S.; Saiz-Lopez, A.; Thornton, J. A.; von Glasow, R. Tropospheric Halogen Chemistry: Sources, Cycling, and Impacts. *Chem. Rev.* **2015**, *115*, 4035–4062.

(20) Galley, R. J.; Babb, D.; Ogi, M.; Else, B. G. T.; Geilfus, N.-X.; Crabeck, O.; Barber, D. G.; Rysgaard, S. Replacement of Multiyear Sea Ice and Changes in the Open Water Season Duration in the Beaufort Sea since 2004. *J. Geophys. Res.: Oceans* **2016**, *121* (3), 1806–1823.

(21) Peterson, P. K.; Simpson, W. R.; Pratt, K. A.; Shepson, P. B.; Frieß, U.; Zielcke, J.; Platt, U.; Walsh, S. J.; Nghiem, S. V. Dependence of the Vertical Distribution of Bromine Monoxide in the Lower Troposphere on Meteorological Factors such as Wind Speed and Stability. *Atmos. Chem. Phys.* **2015**, *15*, 2119–2137.

(22) Liao, J.; Sihler, H.; Huey, L. G.; Neuman, J. A.; Tanner, D. J.; Frieß, U.; Platt, U.; Flocke, F. M.; Orlando, J. J.; Shepson, P. B.; Beine, H. J.; Weinheimer, A. J.; Sjostedt, S. J.; Nowak, J. B.; Knapp, D. J.; Staebler, R. M.; Zheng, W.; Sander, R.; Hall, S. R.; Ullmann, K. A Comparison of Arctic BrO Measurements by Chemical Ionization Mass Spectrometry and Long Path-Differential Optical Absorption Spectroscopy. *J. Geophys. Res.* **2011**, *116* (D14), D00R02.

(23) Neuman, J. A.; Nowak, J. B.; Huey, L. G.; Burkholder, J. B.; Dibb, J. E.; Holloway, J. S.; Liao, J.; Peischl, J.; Roberts, J. M.; Ryerson, T. B.; Scheuer, E.; Stark, H.; Stickel, R. E.; Tanner, D. J.; Weinheimer, A. J. Bromine Measurements in Ozone Depleted Air over the Arctic Ocean. *Atmos. Chem. Phys.* **2010**, *10* (14), 6503–6514.

(24) Guimbaud, C.; Grannas, A. M.; Shepson, P. B.; Fuentes, J. D.; Boudries, H.; Bottenheim, J. W.; Domine, F.; Houdier, S.; Perrier, S.; Biesenthal, T. B.; Splawn, B. G. Snowpack Processing of Acetaldehyde and Acetone in the Arctic Atmospheric Boundary Layer. *Atmos. Environ.* **2002**, *36*, 2743–2752.

(25) Stull, R. B. *An Introduction to Boundary Layer Meteorology*; Berger, A., Crutzen, P. J., Georgii, H.-W., Hobbs, P. V., Hollingsworth, A., Kondratyev, K. Y., Krishnamurti, T. N., Latham, J., Lilly, D. K., London, J., Oort, A. H., Orlanski, I., Pruppacher, H. R., Rosenberg, N. J., Schuurmans, C. J. E., Tennekes, H., Twomey, S. A., Wigley, T. M. L., Wijngaard, J. C., Zuev, V. E., Eds.; Kluwer Academic Publishers: Norwell, MA, 1999.

(26) Nghiem, S. V.; Clemente-Colon, P.; Douglas, T.; Moore, C. W.; Obrist, D.; Perovich, D. K.; Pratt, K. A.; Rigor, I. G.; Simpson, W. R.; Shepson, P. B.; Steffen, A.; Woods, J. Studying Bromine, Ozone, and Mercury Chemistry in the Arctic. *Eos (Washington, DC, U. S.)* **2013**, *94* (33), 289–291.

(27) Boylan, P.; Helmig, D.; Staebler, R.; Turnipseed, A.; Fairall, C.; Neff, W. Boundary Layer Dynamics during the Ocean-Atmosphere-Sea-Ice-Snow (OASIS) 2009 Experiment at Barrow, AK. *J. Geophys. Res.: Atmos.* **2014**, *119*, 2261–2278.

(28) Abbatt, J. P. D.; Oldridge, N.; Symington, A.; Chukalovskiy, V.; McWhinney, R. D.; Sjostedt, S.; Cox, R. A. Release of Gas-Phase Halogens by Photolytic Generation of OH in Frozen Halide-Nitrate Solutions: An Active Halogen Formation Mechanism? *J. Phys. Chem. A* **2010**, *114* (23), 6527–6533.

(29) Wren, S. N.; Donaldson, D. J.; Abbatt, J. P. D. Photochemical Chlorine and Bromine Activation from Artificial Saline Snow. *Atmos. Chem. Phys.* **2013**, *13* (19), 9789–9800.

(30) Albert, M. R.; Grannas, A. M.; Bottenheim, J.; Shepson, P. B.; Perron, F. E. Processes and Properties of Snow-Air Transfer in the High Arctic with Application to Interstitial Ozone at Alert, Canada. *Atmos. Environ.* **2002**, *36* (15–16), 2779–2787.

(31) Colbeck, S. Model of Windpumping for Layered Snow. *J. Glaciol.* **1997**, *43* (143), 60–65.

(32) Adams, J. W.; Holmes, N. S.; Crowley, J. N. Uptake and Reaction of HOBr on Frozen and Dry NaCl/NaBr Surfaces between 253 and 233 K. *Atmos. Chem. Phys.* **2002**, *2*, 79–91.

(33) Huff, A. K.; Abbatt, J. P. D. Kinetics and Product Yields in the Heterogeneous Reactions of HOBr with Ice Surfaces Containing NaBr and NaCl. *J. Phys. Chem. A* **2002**, *106*, 5279–5287.

(34) Kirchner, U.; Benter, T.; Schindler, R. N. Experimental Verification of Gas Phase Bromine Enrichment in Reaction of HOBr

with Sea Salt Doped Ice Surfaces. *Ber. Bunsen-Ges. Phys. Chem.* **1997**, *101* (6), 975–977.

(35) Hu, J. H.; Shi, Q.; Davidovits, P.; Worsnop, D. R.; Zahniser, M. S.; Kolb, C. E. Reactive Uptake of  $\text{Cl}_2(\text{g})$  and  $\text{Br}_2(\text{g})$  by Aqueous Surfaces as a Function of  $\text{Br}^-$  and  $\text{I}^-$  Ion Concentration: The Effect of Chemical Reaction at the Interface. *J. Phys. Chem.* **1995**, *99* (21), 8768–8776.

(36) Ghosal, S.; Shheeb, A.; Hemminger, J. C. Surface Segregation of Bromine in Bromide Doped NaCl: Implications for the Seasonal Variations in Arctic Ozone. *Geophys. Res. Lett.* **2000**, *27* (13), 1879–1882.

(37) Ghosal, S.; Hemminger, J. C.; Bluhm, H.; Mun, B. S.; Hebenstreit, E. L. D.; Ketteler, G.; Ogletree, D. F.; Requejo, F. G.; Salmeron, M. Electron Spectroscopy of Aqueous Solution Interfaces Reveals Surface Enhancement of Halides. *Science (Washington, DC, U. S.)* **2005**, *307* (5709), 563–566.

(38) Gladich, I.; Shepson, P. B.; Carignano, M. A.; Szleifer, I. Halide Affinity for the Water-Air Interface in Aqueous Solutions of Mixtures of Sodium Salts. *J. Phys. Chem. A* **2011**, *115* (23), 5895–5899.

(39) Jungwirth, P.; Tobias, D. J. Molecular Structure of Salt Solutions: A New View of the Interface with Implications for Heterogeneous Atmospheric Chemistry Molecular Structure of Salt Solutions: A New View of the Interface with Implications for. *J. Phys. Chem. B* **2001**, *105* (43), 10468–10472.

(40) Zangmeister, C. D.; Turner, J. A.; Pemberton, J. E. Segregation of NaBr in NaBr/NaCl Crystals Grown from Aqueous Solutions: Implications for Sea Salt Surface Chemistry. *Geophys. Res. Lett.* **2001**, *28* (6), 995–998.

(41) France, J. L.; Reay, H. J.; King, M. D.; Voisin, D.; Jacobi, H. W.; Domine, F.; Beine, H.; Anastasio, C.; Macarthur, A.; Lee-Taylor, J. Hydroxyl Radical and  $\text{NO}_x$  Production Rates, Black Carbon Concentrations and Light-Absorbing Impurities in Snow from Field Measurements of Light Penetration and Nadir Reflectivity of Onshore and Offshore Coastal Alaskan Snow. *J. Geophys. Res.* **2012**, *117* (D14), D00R12.

(42) Sjostedt, S. J.; Abbatt, J. P. D. Release of Gas-Phase Halogens from Sodium Halide Substrates: Heterogeneous Oxidation of Frozen Solutions and Desiccated Salts by Hydroxyl Radicals. *Environ. Res. Lett.* **2008**, *3* (4), 045007.

(43) Burkholder, J. B.; Sander, S. P.; Abbatt, J. P. D.; Barker, J. R.; Huie, R. E.; Kolb, C. E.; Kurylo, M. J.; Orkin, V. L.; Wilmouth, D. M.; Wind, P. H. *Chemical Kinetics and Photochemical Data for Use in Atmospheric Studies*; Jet Propulsion Laboratory (JPL), California Institute of Technology: Pasadena, CA, 2015, Evaluation Number 18, JPL Publication 15-10.

(44) Koop, T.; Kapilashrami, A.; Molina, L. T.; Molina, M. J. Phase Transitions of Sea-Salt/water Mixtures at Low Temperatures: Implications for Ozone Chemistry in the Polar Marine Boundary Layer. *J. Geophys. Res.* **2000**, *105* (D21), 26393–26402.

(45) Knipping, E. M. Modeling  $\text{Cl}_2$  Formation from Aqueous NaCl Particles: Evidence for Interfacial Reactions and Importance of  $\text{Cl}_2$  Decomposition in Alkaline Solution. *J. Geophys. Res.* **2002**, *107* (D18), 4360.

(46) Zelenov, V. V.; Aparina, E. V.; Kashtanov, S. A.; Shestakov, D. V.; Gershenson, Y. M. Kinetic Mechanism of  $\text{ClONO}_2$  Uptake on Polycrystalline Film of NaCl. *J. Phys. Chem. A* **2006**, *110* (21), 6771–6780.

(47) Hausmann, M.; Platt, U. Spectroscopic Measurement of Bromine Oxide and Ozone in the High Arctic during Polar Sunrise Experiment 1992. *J. Geophys. Res.* **1994**, *99* (D12), 25399.

(48) Piot, M.; von Glasow, R. Modelling the Multiphase near-Surface Chemistry Related to Ozone Depletions in Polar Spring. *J. Atmos. Chem.* **2009**, *64* (2–3), 77–105.

(49) Toyota, K.; McConnell, J. C.; Staebler, R. M.; Dastoor, A. P. Air–snowpack Exchange of Bromine, Ozone and Mercury in the Springtime Arctic Simulated by the 1-D Model PHANTAS—Part 1: In-Snow Bromine Activation and Its Impact on Ozone. *Atmos. Chem. Phys.* **2014**, *14* (8), 4101–4133.

(50) Beine, H. J.; Anastasio, C.; Esposito, G.; Patten, K.; Wilkening, E.; Domine, F.; Voisin, D.; Barret, M.; Houdier, S.; Hall, S. Soluble, Light-Absorbing Species in Snow at Barrow, Alaska. *J. Geophys. Res.: Atmos.* **2011**, *116* (18), 1–16.

(51) Jobson, B. T.; Niki, H.; Yokouchi, Y.; Bottenheim, J. W.; Hopper, F.; Leitch, R. Measurements of  $\text{C}_2$ – $\text{C}_6$  Hydrocarbons during the Polar Sunrise 1992 Experiment: Evidence for Cl Atom and Br Atom Chemistry. *J. Geophys. Res.* **1994**, *99* (D12), 25355.